

COMMISSIONING AND RESTART OF ESRF-EBS

S. White, N. Carmignani, L. Carver, J. Chavanne, L. Farvacque, L. Hardy, J. Jacob, G. Le Bec, S. M. Liuzzo, T. Perron, Q. Qin, P. Raimondi, J-L Revol, K. B. Scheidt
European Synchrotron Radiation Facility, Grenoble, France

Abstract

The ESRF operates a 6 GeV 4th generation light source, the ESRF-EBS. This storage ring is the first to implement the Hybrid Multi-Bend Achromat lattice (HMBA). The HMBA lattice provides a reduction of the horizontal emittance of approximately a factor 30 with respect to the former Double Bend Achromat (DBA) structure, considerably improving the brilliance and transverse coherence of the ESRF accelerator complex while maintaining large horizontal acceptance and excellent lifetime performance. In this report, the characteristics of the HMBA lattice will be reviewed and the beam commissioning results and first operation experience of the new ESRF storage ring will be presented.

INTRODUCTION

The ESRF accelerator complex consists of a 200 MeV linac, a 6 GeV booster synchrotron and a 6 GeV storage ring light source [1, 2]. X-ray sources and beam lines are located either in one of the 32 straight sections equipped with undulators (ID beam lines) or in the center of the arcs where the light is extracted from special dipole magnets (BM beam lines). The ESRF upgrade program phase II [2] consists for the most part in replacing the original storage ring operating with 4 nm.rad horizontal emittance with an entirely new machine with the aim of reducing the horizontal emittance down to 133 pm.rad therefore providing a substantial increase of the brilliance and transverse coherence of the photon source.

Table 1: Main Parameters of the ESRF DBA and HMBA Lattices

	Units	DBA	HMBA
E	GeV	6	6
L_{total}	m	844.44	843.98
# cells		32	32
L_{dip}/L_{total}	%	18	38
ϵ_h	pm rad	3985	133
ϵ_v	pm rad	4	1
δ_E	%	0.106	0.094
b_l	mm	3.43	2.9
I_{e-}	mA	200	200
J_x		1.00	1.51
U_0	MeV/turn	4.88	2.56
$\langle \theta \rangle$	rad	0.04	0.020
max. K_{quad}	Tm ⁻¹	16	91
max. K_{sext}	Tm ⁻²	222	1720
max. K_{oct}	Tm ⁻³	0	36025
# magnets/cell		19	32

Table 1 summarizes the main lattice and beam parameters of the two rings. The new storage ring lattice design is based on the Hybrid Multi-Bend Achromat (HMBA) concept introduced in 2012 at the ESRF [3, 4]. This lattice combines several novel concepts with respect to previous proposals allowing for a reduction of a factor 30 in horizontal emittance while maintaining a transverse acceptance compatible with off-axis injection and lifetime of the order of 20 h. In this report, a brief description of the HMBA lattice will be provided followed by a review of the commissioning and first operation experience of the new ESRF storage ring.

THE HMBA LATTICE

The HMBA lattice integrates the Multi-Bend Achromat proposal [5] to increase the number of dipoles, reduce their bending angle and consequently reduce the horizontal emittance. Although proposed in 1995, this concept was first demonstrated in 2015 for a 3 GeV lattice when the MAXIV [6–8] facility started operation. However, adapting this lattice to the 6 GeV ESRF storage ring was found impractical at the time as magnets strengths had to be increased beyond state of the art technology and the transverse and momentum acceptances were found too small to accommodate the standard off-axis injection [3, 9] and large beam lifetime [10, 11]. Recent developments now provide solutions to inject in very small transverse acceptance [12, 13] but these were not considered at the time for the ESRF. Nevertheless, the HMBA lattice introduces novel ingredients that allow to significantly reduce the magnets strengths while improving the acceptance of the lattice and achieving ultra-low emittances [2, 4]. The ESRF HMBA lattice design characteristics can be summarized as follows:

- horizontal equilibrium emittance of 133 pm.rad
- optimized sextupole layout and associated optics functions to reduce their strengths and allow for shorter magnets in order to accommodate the increased number of dipoles while compensating for the large natural chromaticity introduced by high gradient (91 Tm⁻¹) quadrupoles
- intrinsic compensation of non-linear resonances to provide large transverse and momentum acceptances allowing for off-axis injection with more than 90 % efficiency and beam lifetime on the order of 20 h
- reduced overall power consumption provided by the smaller radiated power U_0 and usage of permanent magnet technology for the dipoles

The unit cell of the ESRF HMBA lattice is shown in Fig. 1 and the main ring parameters are summarized in Table 1. The optimized dipole layout and longitudinal gradient allow to increase the β -functions and dispersion at the

Content from this work may be used under the terms of the CC BY 3.0 licence (© 2021). Any distribution of this work must maintain attribution to the author(s), title of the work, publisher, and DOI

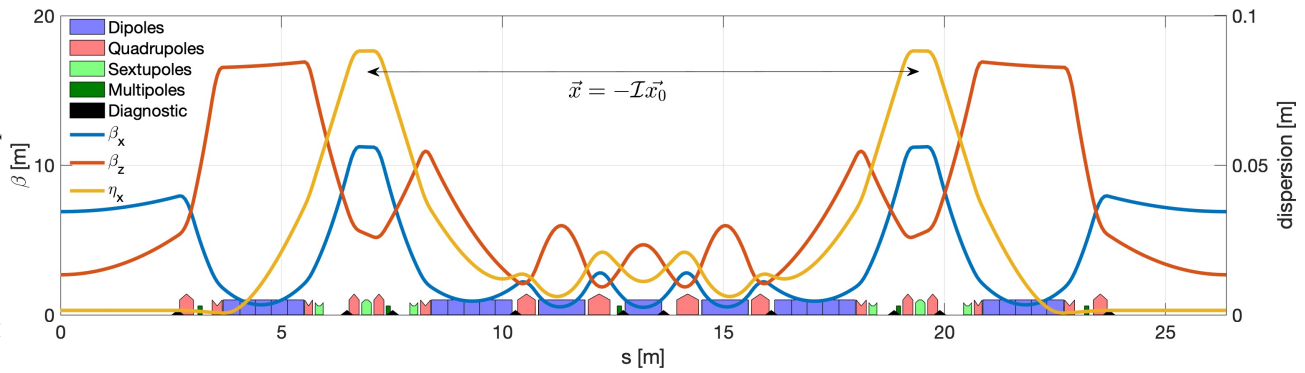


Figure 1: Lattice functions and magnets layout for the HMBA storage ring standard cell.

sextupoles to reduce their strengths and slightly reduce the horizontal emittance [14, 15]. The central part of the cell is composed of strong focusing quadrupoles and defocusing combined dipole-quadrupole magnets to optimize the space usage and increase the horizontal damping partition number J_x ($\epsilon_h \propto J_x^{-1}$). Finally, the HMBA lattice imposes an odd multiple of π phase advance, or $-\mathcal{I}$ transform [16], between focusing sextupoles to partially cancel non-linear resonances [17–19]. This allows to keep magnet strengths compatible with available technologies and increase the filling factor, L_{dip}/L_{total} to reduce the equilibrium emittance without compromising lifetime and transverse acceptance. The horizontal β -function is increased to 18.6 m at the injection point to allow for high efficiency off-axis injection. This breaks the 32-fold symmetry, however, the lifetime performance is back to the design goal of approximately 20 h with appropriate sextupole optimizations [20]. Finally, special bending magnets are introduced in the arcs to extract light into the bending magnet beam lines. A total of 16 such magnets are integrated resulting in a horizontal emittance increase to approximately 140 pm.rad [21].

BEAM COMMISSIONING EXPERIENCE

The ESRF-EBS storage ring beam commissioning took place over a period of 3 months, from the end of November 2019 to the end of February 2020. Two shutdown periods for maintenance were included resulting in a total 2 months integrated beam time. This section provides an overview of the storage ring beam commissioning. A chronological timeline with the commissioning highlights is given for reference in Fig. 2, however only few selected topics can be discussed in this paper. It should be noted, that the success of the beam

commissioning relied heavily on the excellent preparation and readiness of all critical subsystems. A machine simulator was implemented that allowed to develop and test most of the control system and numerical tools well before the start of the commissioning. Based on the solid experience acquired on the previous machine and clever adaptation of many systems the diagnostics, power supplies, RF systems, magnets and their controls provided excellent performance from day one and throughout the whole period.

Injectors Commissioning

In order to comply with a very tight commissioning schedule and to mitigate the overall risks for the project completion it was decided to minimize or anticipate modifications on the injectors chain. In this spirit, a complete refurbishment of the linac, the Booster power supply and RF systems and the renewal of global timing system were performed prior to the dismantling of the old storage ring and the storage ring standard off-axis injection was maintained. However, necessary adaptations of the Booster and transfer lines took place:

- Reduction of the Booster circumference to match the storage ring [2]
- New layout of the transfer lines
- Adaptation of the injection and extraction systems

Although the reduction of the booster circumference represented a major intervention, it was completed according to schedule and the restart of the injectors was completed in a few days. The Booster was foreseen to operate off energy with higher tunes, i.e. new optics, to reduce the horizontal emittance and improve the transfer efficiency. This higher tune optics was not implemented and is under devel-

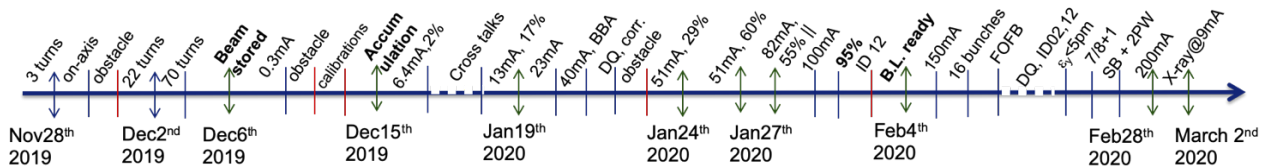


Figure 2: EBS commissioning chronological timeline including main achievements, current, injection efficiency, problems and beam lines highlights.

opment. This was compensated by the implementation of an emittance exchange scheme at the Booster extraction that provided a substantial horizontal beam size reduction [22].

First Turns and Accumulation

Tests and validations of first turns steering performed in the previous machine combined with simulation for the ESRF-EBS indicated that it was possible to establish the closed orbit starting from off-axis injection with all magnets at their design strengths [23]. This strategy was quickly revised as major difficulties were faced during the first weeks of commissioning due to unexpected reductions of both mechanical and dynamic apertures, requiring to minimize injection oscillations. It was later possible to identify and associate these reductions to either physical obstacles inside the vacuum chambers, 3 were found as shown in Fig. 2, or unforeseen large magnetic errors due to cross talk between magnets [24] and wrongly assigned calibration factors [25]. Once these issues were solved the machine performance steadily improved without major difficulties.

First turns could nevertheless be established using off-axis injection and 2.5 turns were achieved without any correction in the storage ring (all correctors off). The first turns trajectory is shown in Fig. 3 where a clear drop in current (pro-

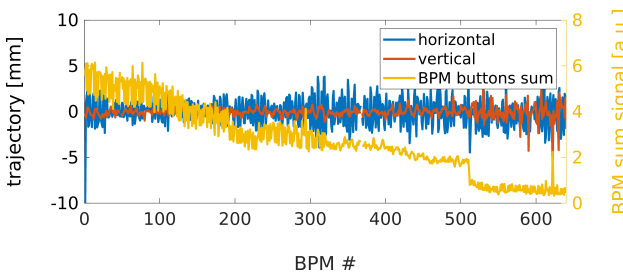


Figure 3: First turns trajectory in the storage ring with off-axis injection.

portional to the BPM sum signal) at approximately 1.5 turns (BPM sample 510, 320 samples per turn) is observed. This was the first clear indication of a physical obstacle later found in straight section 23. At this point, it was impossible to proceed further and it was decided to introduce on-axis injection by combining a static closed orbit bump and increased injection kickers strengths. In these conditions, it was possible to progress with beam threading and establish multiple turns, however in order to achieve the 70 turns required to turn on the RF systems and allow for capture, sextupole magnets adjustments proved to be essential. This is shown in Fig. 4 where the BPM sum signal is shown as a function of turns. The blue line, featuring a plateau at low turn numbers, corresponds to the settings optimized for first turns, the black line the design settings and the red line the settings optimized for RF capture that were defined based on tracking simulations of survival rate in realistic conditions.

Beam accumulation is not possible with on-axis injection, the injection kickers were therefore optimized to share oscillations between the stored and injected beams and allow to inject in the reduced acceptance. A maximum total cur-

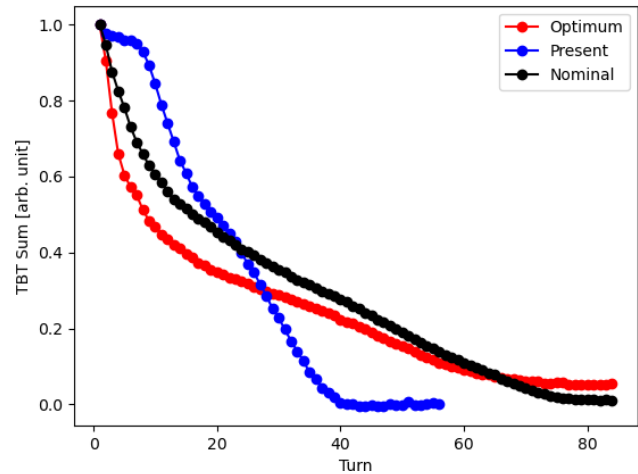


Figure 4: Measured turn by turn sum signal from BPM 5 of cell 7 for different sextupole settings iterations

rent of 6 mA was accumulated with an injection efficiency of 0.8 % before the Christmas break 2020. Following this initial commissioning period, the magnetic model was improved to include cross-talks and calibrations factors were properly assigned. It was then possible to perform closed orbit correction, optics tuning and proceed with the ramp in current and vacuum conditioning.

Closed Orbit and Optics Corrections

The initial rms closed orbit of several hundred microns was in large part due to uncorrected offsets and could be reduced down to approximately 50 μm rms in both planes after the beam based alignment and the introduction of a large number of singular vectors in the correction loop.

Figure 5 shows the result of the beam based alignment campaign, rms offsets of approximately 100 μm were found in both planes. It should be noted that electronic and mechanical offset corrections were applied before the start of commissioning. The orbit correction is performed using standard Singular Value Decomposition (SVD) methods. The optimal number of singular vectors to minimize β -beating and increasing dynamic aperture was determined to be 162 in both planes with numerical simulations including realistic alignment errors [25]. Pushing to higher values would result in significant increase in corrector strengths with very minor performance improvement.

Optics measurements and corrections were done using the Orbit Response Matrix (ORM) method. Although large magnetic errors were initially present, measurements were performed very early in the commissioning. Initial rms β -beating of 20 % and 34 % and dispersion mismatch of 23.6 mm and 4.3 mm in the horizontal and vertical planes respectively were estimated from these measurements. After the magnetic and lattice models were corrected the optics corrections converged to $\Delta\beta/\beta \approx 1.5\%$ in both planes and $\Delta\eta \approx 2.0$ mm and 1 mm in the horizontal and vertical planes respectively [25]. All gradient corrections are applied on quadrupole magnets located in the direct vicinity of sex-

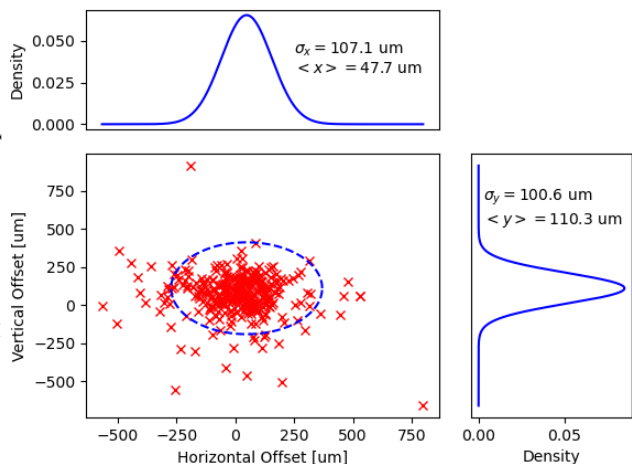


Figure 5: Measured BPM offsets in the horizontal and vertical planes. The blue dashed line is placed at 3σ .

tupoles. This shows that optics errors are for the most part dominated by the feed-down effects in sextupole magnets driven by non-zero closed orbit at their location, as expected from the model, and demonstrates that the construction, magnetic measurements and modeling of the lattice magnets is very accurate and that no strong calibration or unexpected localized errors were left in the machine. The integration of BM beam-lines did not introduce any additional errors [25]. Coupling and vertical dispersion corrections are also derived from ORM measurements. Measured emittances of $130 \pm 20 \text{ pm.rad}$ and below $1 \pm 1 \text{ pm.rad}$ are measured after coupling corrections without any further tuning. However these values may suffer large errors bars associated with the resolution and calibration of the pinhole cameras. In User Service Mode (USM), the vertical emittance is stabilized at 10 pm.rad using a feedback loop injecting white noise. It is therefore not sensitive to small drifts or variations related to gap movements and orbit fluctuations.

Table 2: rms Storage Ring Corrections

	Units	Simulations	SR
θ_h	μrad	160	65
θ_v	μrad	120	30
$\Delta K_1/K_1$	%	0.26	0.2

Table 2 compares the applied and expected correction strengths needed to achieve the results from Table 3. In all cases, applied strengths are lower than model predictions. This clearly reflects the outstanding work done during the engineering, construction and installation of the ESRF-EBS storage ring. Alignment errors can be estimated from these using a simplified model. As shown in Fig. 6, the estimated errors range from 25 to $45 \mu\text{m}$ in the horizontal plane and from 25 to $35 \mu\text{m}$ in the vertical plane. This is much better than the specifications of 65 and $55 \mu\text{m}$ in the horizontal and vertical plane respectively. These estimates are very approximate. However, injection was possible without any

Table 3: Design and Delivered Parameters in USM Condition and Uniform Mode. The Design Lifetimes were Rescaled for 10 pm.rad Vertical Emittance for Comparison Purpose.

	Units	Design	Delivered
I_e	mA	200	200
Inj. Eff.	%	>90	80
Vacuum LT	h	300	122 ± 13
Touschek LT	h	28	41 ± 5
USM LT	h	23	25
ϵ_h	pm.rad	140	$<130 \pm 20$
ϵ_v	pm.rad	10	10 ± 1
rms orbit (x,y)	μm	140, 80	50, 55
Stability	σ	0.05	<0.01

corrections and 26 out of the 27 ID beam lines could see light without adjustments on the very first trial to open the front-ends. Both these observations confirm the excellent alignment of the machine.

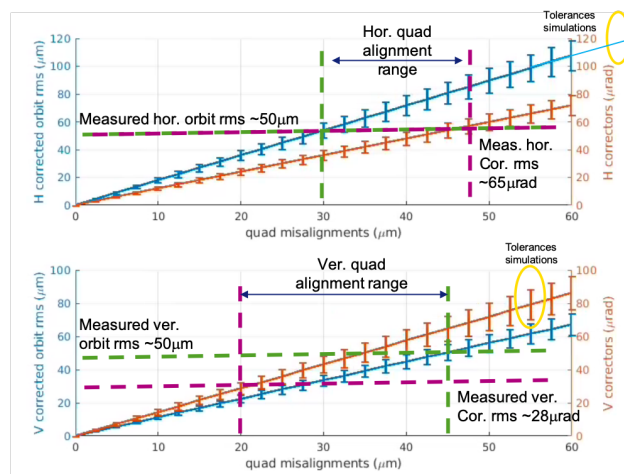


Figure 6: Estimated storage ring alignment errors from simulations.

DELIVERED PARAMETERS AND FIRST OPERATION EXPERIENCE

The initial commissioning allowed to remove all physical obstacles and substantially increase the machine acceptance. The final one, that represented the last major difficulty on the way to deliver operating conditions compatible with the start of beam lines commissioning, was removed 2 months after the start of commissioning. After that, conditions were established for current ramp-up. Efficient conditioning of the vacuum chambers and the RF cavities to increasing beam loading [26, 27] allowed to achieve the nominal current of 200 mA before the end of the beam commissioning period.

Table 3 compares the design and delivered beam and machine parameters. The results are excellent and matching or exceeding design goals in all aspects except for injection

efficiency. The horizontal emittance fluctuates between 120 and 130 pm.rad depending on insertion devices gap settings and the vertical emittance is fixed at 10 pm.rad to increase the lifetime as for the moment no significant improvement in performance was observed by the beamlines going to lower values. This value will be re-evaluated in the future.

The beam stability is measured with all feed-backs running on a short timescale, long term stability is being evaluated. 3 lifetime values are quoted in this paper: the vacuum lifetime evaluated with vertical emittance scans, the Touschek lifetime rescaled to 10 pm for the design and measured with all gaps and collimators opened on a fully optimized machine and the USM lifetime which corresponds to the average lifetime delivered at 200 mA over one week of uniform. This value is reduced by approximately 10% by the collimation systems [28] used to localized Touschek losses in shielded areas. While the vacuum lifetime remains a bit low, showing the need for further conditioning, the Touschek lifetime exceeds model predictions of 28 h. This is partly explained by the excellent alignment as shown in Fig. 6 but also the result of the optimization of a large set of parameters, such as tunes, RF voltage or skew quadrupoles, sextupoles and octupoles strengths. These optimizations took place on a regular basis during the vacuum conditioning and significant changes were applied in some cases as the beam and vacuum conditions were improving. With all these optimizations integrated in the operation settings, lifetime tuning for USM now relies on online optimizations that consist in minimizing the losses measured by the Beam loss Detector (BLD) system by scanning individual sextupoles, octupoles and skew quadrupoles. The implementation of individual power supplies for all these magnets as part of the ESRF storage ring upgrade therefore proves to be essential for performance optimization. These are performed on a regular basis and after each shutdown period to maintain a lifetime >20h at 200 mA. With a fully optimized storage ring, the machine operates routinely with ID gaps closed at an injection efficiency of approximately 80%. The measured on-momentum dynamic aperture is smaller than model prediction by 1 mm which could explain the lower than expected injection efficiency. This observation combined with larger than expected lifetime could indicate that excessive weight was put on lifetime in the optimization process.

The lattice performance after one year of operation is excellent [29], however, two major issues remain to be solved:

- overheating of the ceramic chambers limits the current for the timing modes
- the injection systems do not provide transparent injection and beam line experiments are perturbed

Single bunch collective effects have been evaluated and are for the most part consistent with the impedance model predictions [30]. They do not limit the single bunch current as the maximum design value of 10 mA could easily be achieved with either increased chromaticity or bunch-by-bunch feedback. However, beam induced heating on the ceramic chambers generates excessive mechanical stress that the present design cannot sustain. The procurement of new

more robust ceramic chambers was launched for installation at the end of the year. This issue presently limits the single bunch current to 4 mA and the total current of the 16 bunch mode to 1/3 of its nominal value.

Injection perturbations have been a major concern since the introduction of top-up operation at ESRF in 2016. Quasi-transparent injection was achieved in the previous machine [31] and equivalent oscillation amplitudes are obtained in the ESRF-EBS making use of the existing feed-forward systems. However when normalized to the beam size, these perturbation are an order of magnitude larger than in the previous machine. Corrective actions, including the installation of new kicker power supplies and the integration of advanced injection systems for on-axis injection are presently under development [32, 33].

CONCLUSION

The ESRF HMBA lattice was designed to match strict constraints imposed by the in-place infrastructure such as the tunnel and beam lines locations and number. The performance and results presented in this report exceed by far our expectations and denote the original design of this lattice. However, several issues remain that presently limit the performance reach of the accelerator complex and need to be addressed. Finally, room is left for further improvements based on our growing understanding of the lattice. Reduction of the photon source size by redistributing the damping partition number and better matching of the β -functions in straight sections while increasing the acceptance of the machine with better matching of the optics off-energy is within reach and studies are ongoing in this direction.

ACKNOWLEDGEMENTS

This work is the result of the commitment of not only the ASD staff members, who we warmly thank, but also of all the supporting divisions and groups at ESRF. We are really grateful to ISDD, TID and the Experiment Division for their invaluable contributions throughout the project. We also would like to thank the MAC and its members for their useful advice and support.

REFERENCES

- [1] ESRF foundation, “ESRF foundation phase report (Red book)”, ESRF, Grenoble, France, Rep. ESRF, 1987.
- [2] D. Andrault *et al.*, “ESRF upgrade programme phase II (Orange Book)”, ESRF, Grenoble, France, Rep. ESRF, 2014.
- [3] L. Farvacque *et al.*, “A Low-Emittance Lattice for the ESRF”, in *Proc. IPAC'13*, Shanghai, China, May 2013, paper MO-PEA008, pp. 79–81.
- [4] J. C. Biasci *et al.*, “A low emittance lattice for the ESRF”, *Synchrotron Radiation News*, vol. 27, pp. 8–12, 2014. doi: 10.1080/08940886.2014.970931
- [5] D. Einfeld, J. Schaper, and M. Plesko, “Design of a diffraction limited light source (DIFL)”, vol. 1, pp. 177 - 179, 1995. doi: 10.1109/PAC.1995.504602

- [6] P. F. Tavares *et al.*, “Commissioning and first-year operational results of the MAX IV 3 GeV ring”, *J. Synch. Radiat.*, vol. 25, pp. 1291–1316, 2018. doi:10.1107/S1600577518008111
- [7] H. Tarawneh *et al.*, “MAX-IV lattice, dynamic properties and magnet system”, *Nucl. Instrum. Meth. A*, vol. 508, pp. 480–486, 2003. doi:10.1016/S0168-9002(03)01699-1
- [8] M. Magnuson *et al.*, “MAX IV conceptual design report (CDR)”, Max IV, Lund, Sweden, Rep. CDR, 2006.
- [9] A. Chao and M. Tigner, *Handbook of Accelerator Physics and Engineering*. Singapore: World Scientific, 1999.
- [10] P. Elleaume, “The ultimate hard X-ray storage-ring-based light source”, *Nucl. Instrum. Meth. A*, vol. 500, pp. 18–24, 2003. doi:10.1016/S0168-9002(03)00737-X
- [11] Y. Cai *et al.*, “Ultimate storage ring based on fourth-order geometric achromats”, *Phys. Rev. ST Accel. Beams*, vol. 15, p. 054002, 2012. doi:10.1103/PhysRevSTAB.15.054002
- [12] V. Sajaev, “Commissioning simulations for the Argonne Advanced Photon Source upgrade lattice”, *Phys. Rev. Accel. Beams*, vol. 22, p. 040102, 2019. doi:10.1103/PhysRevAccelBeams.22.040102
- [13] C. Steier *et al.*, “Completion of the brightness upgrade of the ALS”, *IOP Journal of Physics*, vol. 493, p. 012030, 2014. doi:10.1088/1742-6596/493/1/012030
- [14] S. Papadopoulou, F. Antoniou, and Y. Papaphilippou, “Emitance reduction with variable bending magnet strengths: Analytical optics considerations and application to the Compact Linear Collider damping ring design”, *Phys. Rev. Accel. Beams*, vol. 22, p. 091601, 2019. doi:10.1103/PhysRevAccelBeams.22.091601
- [15] R. Nagaoka and A. Wrulich, “Emittance minimisation with longitudinal dipole field variation”, *Nucl. Instrum. Meth. A*, vol. 575, pp 292-304, 2007. doi:10.1016/j.nima.2007.02.086
- [16] H. Wiedemann, *Particle Accelerator Physics*. Switzerland: Springer International Publishing, 2007.
- [17] P. Raimondi and A. Seryi, “A novel final focus design for future linear colliders”, *Phys. Rev. Lett.*, vol. 86, p. 3779, 2001. doi:10.1103/PhysRevLett.86.3779
- [18] M. Bona *et al.*, “SuperB: A High-luminosity asymmetric e+ e- super flavor factory. conceptual design report”, SLAC, Menlo Park, CA, USA, SLAC-R-856, May 2007.
- [19] K. Oide *et al.*, “Design of beam optics for the future circular collider e+e- collider rings”, *Phys. Rev. Accel. Beams*, vol. 19, p. 111005, 2016. doi:10.1103/PhysRevAccelBeams.19.111005
- [20] N. Carmignani, *Touschek lifetime studies and optimization of the European Synchrotron Radiation Facility*. Switzerland: Springer International Publishing, 2016. doi:10.1007/978-3-319-25798-3
- [21] S. M. Liuzzo, N. Carmignani, J. Chavanne, L. Farvacque, B. Nash, and P. Raimondi, “Optics Adaptations for Bending Magnet Beam Lines at ESRF: Short Bend, 2-Pole Wiggler, 3-Pole Wiggler”, in *Proc. IPAC’17*, Copenhagen, Denmark, May 2017, pp. 666–669. doi:10.18429/JACoW-IPAC2017-MOPIK062
- [22] N. Carmignani, L. R. Carver, S. M. Liuzzo, T. P. Perron, and S. M. White, “Operation of the ESRF Booster with the New EBS Storage Ring”, presented at IPAC’21, Campinas, Brazil, May 2021, paper MOPAB051, this conference.
- [23] S. Liuzzo *et al.*, “Preparation of the EBS beam commissioning”, *J. Phys. Conf. Ser.*, vol. 1350, p. 012022, 2019. doi:10.1088/1742-6596/1350/1/012022
- [24] G. Le Bec *et al.*, “Crosstalks between storage ring magnets at the Extremely Brilliant Source storage ring at the European Synchrotron Radiation Facility”, submitted for publication, 2021.
- [25] S. M. Liuzzo *et al.*, “HMBA Optics Correction Experience at ESRF”, presented at IPAC’21, Campinas, Brazil, May 2021, paper TUPAB048, this conference.
- [26] J. Jacob, P. B. Borowiec, A. D’Elia, G. Gautier, and V. Serriere, “ESRF-EBS 352.37 MHz Radio Frequency System”, presented at IPAC’21, Campinas, Brazil, May 2021, paper MOPAB108, this conference.
- [27] A. D’Elia, J. Jacob, and V. Serriere, “ESRF-EBS 352 MHz HOM Damped RF Cavities”, presented at IPAC’21, Campinas, Brazil, May 2021, paper MOPAB333, this conference.
- [28] R. Versteegen *et al.*, “Collimation scheme for the ESRF Upgrade”, in *Proc. IPAC’15*, Richmond, VA, USA, May 2015, pp. 1434–1437. doi:10.18429/JACoW-IPAC2015-TUPWA017
- [29] J.-L. Revol *et al.*, “ESRF-EBS: Implementation, Performance and Restart of User Operation”, presented at IPAC’21, Campinas, Brazil, May 2021, paper THPAB074, this conference.
- [30] L. R. Carver *et al.*, “Single Bunch Collective Effects in the EBS Storage Ring”, presented at IPAC’21, Campinas, Brazil, May 2021, paper MOPAB117, this conference.
- [31] S. White *et al.*, “Damping of injection perturbations at the European Synchrotron Radiation Facility”, *Phys. Rev. Accel. Beams*, vol. 22, p. 032803, 2019. doi:10.1103/PhysRevAccelBeams.22.032803
- [32] S. M. White, N. Carmignani, M. Dubrulle, M. Morati, and P. Raimondi, “Transparent Injection for ESRF-EBS”, in *Proc. IPAC’19*, Melbourne, Australia, May 2019, pp. 78–81. doi:10.18429/JACoW-IPAC2019-MOPGW008
- [33] S. M. White *et al.*, “A Flexible Injection Scheme for the ESRF-EBS”, presented at IPAC’21, Campinas, Brazil, May 2021, paper MOPAB116, this conference.